AUXILIARY EJECTOR EFFECTS ON ROCKET-DRIVEN DIFFUSER PERFORMANCE DURING THRUST VARIATION

By

James W. Hale

Rocket Test Facility

ARO, Inc.

TECHNICAL DOCUMENTARY REPORT NO. AEDC-TDR-63-188

September 1963

Program Element 62405184/6950

(Prepared under Contract No. AF 40(600)-1000 by ARO, Inc., contract operator of AEDC, Arnold Air Force Station, Tenn.)

ARNOLD ENGINEERING DEVELOPMENT CENTER

AIR FORCE SYSTEMS COMMAND

UNITED STATES AIR FORCE

NOTICES

Qualified requesters may obtain copies of this report from DDC, Cameron Station, Alexandria, Va. Orders will be expedited if placed through the librarian or other staff member designated to request and receive documents from DDC.

When Government drawings, specifications or other data are used for any purpose other than in connection with a definitely related Government procurement operation, the United States Government thereby incurs no responsibility nor any obligation whatsoever; and the fact that the Government may have formulated, furnished, or in any way supplied the said drawings, specifications, or other data, is not to be regarded by implication or otherwise as in any manner licensing the holder or any other person or corporation, or conveying any rights or permission to manufacture, use, or sell any patented invention that may in any way be related thereto.

AUXILIARY EJECTOR EFFECTS ON ROCKET-DRIVEN DIFFUSER PERFORMANCE DURING THRUST VARIATION

By

James W. Hale

Rocket Test Facility

ARO, Inc.

a subsidiary of Sverdrup and Parcel, Inc.

September 1963

ARO Project No. RT2000

AF - AEDC
Arnold AFS Tenn

ABSTRACT

A model study was made on rocket tailoff, using both annular-type and centerbody-type auxiliary ejectors. The investigation was conducted in the T-5BR1 Altitude Test Cell with steam and air as the driving fluids for both the simulated rocket and annular or centerbody-type ejector. Performance was obtained for the simulated rocket and ejector running individually as a diffuser-ejector and for both the simulated rocket and ejector operating in tandem. The ejector was used to evacuate the test cell prior to simulated rocket ignition and to maintain cell pressure following simulated rocket tailoff.

Both the centerbody-type and annular-type auxiliary ejectors have the effect of a variable area contraction in the diffuser similar to a second throat. The start and breakdown pressure ratio was increased by increasing the ejector driving pressure, which is similar to the effect of reducing the contraction area ratio, A_{st}/A_d, of a second-throat diffuser.

PUBLICATION REVIEW

This report has been reviewed and publication is approved.

Eules L. Hively
Eules L. Hively
Acting Chief, Propulsion Division
DCS/Research

D. R. Eastman, Jr.
Donald R. Eastman, Jr.
DCS/Research

CONTENTS

TABLE

ILLUSTRATIONS

NOMENCLATURE

A_d	Cross-sectional area of diffuser, in.^{2}
A_{ne}	Cross-sectional area of nozzle exit, in.^{2}
A_{st}	Cross-sectional area of second-throat duct, in.^{2}
A^*	Cross-sectional area of nozzle throat, in.^{2}
D	Diameter of diffuser duct, in.
d	Diameter of diffuser second-throat duct, in.
L	Length of diffuser duct at diameter, D, in.
ℓ	Length of diffuser second-throat duct, d, in.
p_c	Test cell pressure, psia
p_{ex}	Diffuser duct exit pressure, psia
p_t	Chamber or total pressure, psia
p_{te}	Ejector driving or total pressure, psia
p_{tr}	Simulated rocket driving or total pressure, psia
T_{te}	Ejector driving fluid total temperature, °R
T_{tr}	Simulated rocket driving fluid total temperature, °R
θ_n	Nozzle divergent half angle, deg

SUBSCRIPTS

act	Actual
isen	Isentropic

1.0 INTRODUCTION

Ground facilities present a problem of maintaining constant simulated altitude conditions for testing rockets throughout the firing sequence, which includes the ignition and tailoff phases. The mass flow from the rocket during the ignition and tailoff phases varies with the rocket driving pressure. Since the test cell pressure is directly proportional to the rocket driving pressure when the diffuser is started and since it depends both on rocket driving pressure and diffuser exit pressure when the diffuser is not started, a constant test cell pressure is impossible to maintain. As long as the diffuser remains started, the ratio of cell-to-rocket driving pressure remains constant, and the change in test cell pressure as a result of a change in rocket driving pressure is small compared with the large increase in test cell pressure during ignition before the diffuser starts and during tailoff after the diffuser breaks down.

Because reduction of this ignition and tailoff peak in test cell pressure is of primary interest, a model study was conducted to determine if the instantaneous test cell pressure peak could be controlled for a rocket tailoff by using either a centerbody-type or annular-type auxiliary ejector. The test was conducted in the Rocket Test Facility (RTF), Arnold Engineering Development Center (AEDC), Air Force Systems Command (AFSC), from February 22 to April 4, 1963.

The auxiliary-type ejector has been used primarily to evacuate the test cell prior to rocket ignition and to maintain cell pressure following rocket tailoff. Both the centerbody-type and the annular-type ejectors allowed the rocket diffuser to remain started at a higher diffuser exit pressure. The level of the diffuser exit pressure at breakdown depended on the level of the auxiliary ejector driving pressure. An increase in ejector driving pressure resulted in an increase in diffuser exit pressure at breakdown. Both types of ejectors were successful in reducing the peak pressure on ignition and tailoff, with the annular-type being the more promising. The apparent advantage of the annular-type ejector over the centerbody-type ejector is that there is no obstruction in the center of the diffuser like the centerbody that produces shock systems (high losses) in the high velocity jet stream from the rocket nozzle which may be supersonic, sonic, or high subsonic even after the pumping action of the rocket-driven diffuser has broken down. If this trailing mass does not suffer the severe losses that are experienced with the centerbody-type

Manuscript received August 1963.

ejector through strong bow shocks, it has more energy when it reaches the ejector jet stream for entrainment. This jet stream imparts additional energy to the slower moving molecules that come from the rocket, which prevent the test cell pressure from reaching the high peak that is normally reached after diffuser breakdown for the centerbody-type ejector.

Correlation of model data and one-dimensional isentropic relationship between duct-to-nozzle throat area ratio, cell-to-nozzle total pressure ratio, diffuser-exit-to-nozzle total pressure ratio, and ratio of specific heats is shown.

2.0 APPARATUS

The two basic diffuser-ejector configurations tested were driven by the same axisymmetric simulated rocket nozzle concentrically located. One of two types of auxiliary ejectors (annular or centerbody) was used in tandem with the simulated rocket.

2.1 SIMULATED ROCKET NOZZLE PLENUM SECTION

A 4-in. schedule 160 pipe 15-3/8 in. long welded to a 12-in. flange was used as the simulated rocket nozzle plenum chamber. The simulated rocket nozzle was installed on the plenum chamber by means of an adapter head as shown in Fig. 1. The nozzle plenum section was located in a sealed plenum or test cell section to which the diffuser was attached. Typical test configurations are shown in Figs. 2a-c.

2.2 SIMULATED ROCKET NOZZLE

The axisymmetric 13.25-deg, half-angle conical nozzle had an exit-to-throat area ratio $A_{ne}/A^* = 12.25$ and a throat diameter of 0.50 in. Dimensional details of this nozzle are presented in Fig. 3.

2.3 SIMULATED ROCKET TEST CELL

The test cell consists of a duct 12 in. in diameter and 21.00 in. long, to which the 24-in.-long diffuser is attached at the downstream end connecting the test cell to the 20-in.-diam exhaust ducting.

2.4 DIFFUSER

The two types of diffusers used were the constant area straight diffuser and the second-throat diffuser. The constant area straight diffuser was used with and without a centerbody-type auxiliary ejector (Figs. 2a and b). The constant area diffuser was a flanged 4.032-in. duct, 24 in. long (see Fig. 4). Inside this straight diffuser was installed concentrically the centerbody-type auxiliary ejector. This test installation is presented in Fig. 2b.

The annular-type ejector nozzle consisted of a conical section placed 1.85 in. downstream of the inlet, forming the transition to the zero length second throat. The ejector nozzle throat consisted of 100 holes 0.0595 in. in diameter (53 wire gage size) by 0.468 in. long (the wall thickness of the diffuser) equally spaced on the circumference of the diffuser near the intersection of the diffuser on the downstream side with the conical section. A manifold around the diffuser enclosing the 100-hole throat supplied the driving fluid to the nozzle. Details of the diffuser and annular-type nozzle are presented in Fig. 5.

2.5 CENTERBODY-TYPE EJECTOR

The centerbody-type ejector consisted of a 30-deg, total-angle nose cone and a 10-deg, half-angle conical nozzle. The nozzle had a 1.118-in. throat diameter through which a 1-in. outside diameter tube extended to supply the driving fluid to the nozzle plenum. This left an annular area of 0.1963 $in.^2$ for the nozzle throat. The nozzle area ratio was $A_{ne}/A^* = 7.54$ based on the reduction in area by the one-inch tube. The centerbody projected area gave a 25.54-percent blockage in the 4.032 in. duct. This blockage is representative of the present RTF ejector installations. Dimensional details of the centerbody-type ejector are presented in Fig. 6.

2.6 SIMULATED ROCKET NOZZLE AND EJECTOR DRIVING FLUID

Air from the VKF 4000-psi storage tank or 200-psig saturated steam from the AEDC central plant provided the driving media for the simulated rocket and auxiliary ejector which discharged to the RTF exhaust machines. A plenum total pressure range from 0 to 412 psia for air and 0 to 198 psia for steam was supplied to the rocket nozzle and/or the ejector nozzle. The diffuser exhaust pressure was varied from 0.27 to 8.95 psia by means of a 20-in., hand-operated gate valve (Fig. 2) or held constant at a predetermined value by the exhaust machines.

2.7 INSTRUMENTATION

The parameters of primary interest were cell pressure, diffuser exit pressure, simulated rocket and ejector plenum total pressure, and the rocket and ejector driving fluid total temperature.

All pressures were read on diaphragm-activated dial gages and recorded on strip charts by a null-balance, potentiometer-type recorder from which the pressures were sensed by transducers. The gages were periodically calibrated, and the readings were well within the calibration range. The temperatures were measured with copper-constantan thermocouples and read on compensating millivolt meters. Both steady-state and transient data were taken.

3.0 TEST PROCEDURE

At the beginning of each test, a vacuum check was made to detect any possible leaks into the system before any data were taken.

The test objective was to determine the rocket start and tailoff diffuser performance when operated in tandem with either a centerbody or annular-type auxiliary ejector. The simulated rocket exhaust discharged into the 4.032-in. constant area straight diffuser (1) without the centerbody ejector installed (Fig. 2a), (2) with the centerbody ejector installed but not running (Fig. 2b), and (3) with the centerbody ejector installed and running. The simulated rocket exhaust also discharged into the second-throat diffuser with the annular ejector not running and running (Fig. 2c). Various combinations were tested in relation to nozzle driving fluids. These combinations are as follows:

Nozzle	Driving Fluids		
Simulated Rocket	air	air	steam
Auxiliary Ejector	steam	air	air

The performance was determined for the simulated rocket and ejectors individually and together for the different driving fluids. The individual performance was determined in accordance with Refs. 1 and 2.

When the simulated rocket and auxiliary ejector were operated together, the exhaust pressure was set at a value approximately equal to 0.8 times the exhaust pressure necessary to maintain the diffuser started when the simulated rocket was operating individually. The auxiliary ejector driving pressure was set at a value approximately

5 psi above the minimum driving pressure necessary for the auxiliary ejector alone to remain started when driving the diffuser with the above exit pressure. Rocket tailoff and ignition were simulated by both a stepwise and a continuous decrease to zero and increase to the original operating value in simulated rocket driving pressure. Simulated rocket tailoff and ignition were also made with P_{ex} held constant, while the auxiliary ejector driving pressure was reduced below that necessary to keep the auxiliary ejector-driven diffuser started when the simulated rocket was not running.

4.0 RESULTS AND DISCUSSION

4.1 INDIVIDUAL ROCKET AND AUXILIARY EJECTOR-DRIVEN, DIFFUSER-EJECTOR PERFORMANCE

The diffuser-ejector performance was obtained individually for both air and steam driving fluids for the simulated rocket nozzle, centerbody-type ejector nozzle, and the annular-type ejector nozzle. The individual performance curves are presented in Fig. 7. The simulated rocket-driven diffuser and the centerbody-type, ejector-driven diffuser gave essentially the same cell-to-driving pressure ratio corresponding to the driving fluid ($P_c/P_t = 0.0015$ for steam driving fluid and $0.0005 \leq P_c/P_t \leq 0.0006$ for air driving fluid). This approximate equality in P_c/P_t was expected since both the simulated rocket nozzle and centerbody-type ejector nozzle were approximately the same size. The nozzle throat areas were equal (0.1963 in.^{2}) and the nozzle area ratios, A_{ne}/A^*, were 12.25 for the simulated rocket nozzle and 7.54 for the centerbody-type ejector nozzle. The half-angles, θ_n, of the simulated rocket nozzle and the centerbody-type ejector nozzle were 13.25 deg (Fig. 3) and 10 deg (Fig. 6), respectively.

The variation in P_c/P_t for the simulated rocket-driven diffuser (0.00055) and the centerbody-type, ejector-driven diffuser (0.0005) with air driving fluid was probably a result of the centerbody-type ejector nozzle having a smaller divergent half angle than did the rocket nozzle. Reference 2 shows that a small half-angle nozzle pumps a lower P_c/P_t ratio than does a large half-angle nozzle.

The scatter in the steam driving fluid data for the rocket and centerbody-type, ejector-driven diffusers was such that no difference could be detected in the P_c/P_t ratios. The scatter was a result of having a very wet (two phase) driving fluid.

Since a common diffuser was used for both simulated rocket and centerbody-type ejector nozzles, the duct-to-nozzle area ratios were

approximately equal (A_d/A^* = 65.05 for the rocket nozzle and 61.03 for the centerbody-type ejector nozzle). The difference in the two ratios was a result of the centerbody-type ejector feed tube area not being considered for the centerbody-type ejector. These air- and steam-driven, diffuser-ejector P_c/P_t ratios are in good agreement with the trend presented in Ref. 3.

The simulated rocket-driven, second-throat diffuser pumped a P_c/P_t ratio of 0.0006, which is higher than the P_c/P_t pumped by the simulated rocket-driven straight diffuser with and without the auxiliary centerbody-type ejector installed. This difference in P_c/P_t ratios may be a result of a slight variation in size of the second-throat diffuser and the straight diffuser and a possible leakage into the test cell. The position of the beginning of the second throat from the nozzle exit must be great enough so that the jet boundary will not impinge on the second-throat transition. Therefore, the beginning of the second throat was positioned so that the intersection of the jet boundary calculated by the method given in Ref. 4 with the diffuser was approximately 0.30 in. upstream of the beginning of the second throat.

The driving pressure ratios, P_{ex}/P_t, at start and breakdown corresponding to the simulated rocket, the auxiliary centerbody ejector, and the annular ejector are presented for steam and air driving fluids in Table 1. The ratios, P_{ex}/P_t, for the auxiliary centerbody-type ejector diffuser installation are lower for both driving fluids than the corresponding ratios for the simulated rocket diffuser installation. This was expected according to Refs. 1 and 5 since the length to diameter ratio, L/D, for the auxiliary ejector-diffuser installation (3.70) was smaller than the L/D for the simulated rocket diffuser installation (6.26). The P_{ex}/P_t ratios for the simulated rocket-driven diffuser with air and steam driving fluids when the auxiliary centerbody-type ejector was installed but not running are in agreement with the trend presented in Fig. 11 of Ref. 3 and Fig. 10 of Ref. 1. The auxiliary centerbody-type ejector blockage (25.54 percent) acts as a second throat in the diffuser and resulted in an improvement in P_{ex}/P_t from 0.0183 to 0.0205 by allowing the jet boundary to fill the duct at a higher diffuser exit pressure.

The annular-type ejector (with a throat of 100 holes, 0.0595 in. in diameter) had a physical throat area of A^* = 0.2781 in.^{2}, which was much larger than the centerbody-type ejector nozzle physical throat area (A^* = 0.1963 in.^{2}). This annular-type nozzle throat area of A^* = 0.2781 in.^{2} with a duct area A_d = 12.77 in.^{2} (D = 4.032 in.) gives an A_d/A^* = 45.92. The P_c/P_t performance of the annular-type, ejector-driven diffuser was much greater than the one-dimensional isentropic

P_c/P_t (Ref. 6) and even greater than the centerbody-type, ejector-driven diffuser P_c/P_t performance. The ratio of P_c/P_t to the isentropic ratio for the centerbody-type, ejector-driven diffuser and annular-type ejector-driven diffuser for their respective physical area ratios, A_d/A^*, are as follows:

Type Ejector	A_d/A^*	$\frac{(P_c/P_t)_{act}}{(P_c/P_t)_{isen}}$	
		Steam	Air
Centerbody-type	61.03	1.871	0.957
Annular-type	45.92	4.277	3.272

The large difference in P_c/P_t for the centerbody-type and annular-type ejectors was probably caused by the difference in A_d/A^* and the difference in pressure losses through the two types of nozzles. The annular-type, ejector-driven diffuser configuration had the smaller physical A_d/A^*, which could account for a part of the higher P_c/P_t obtained. Since the driving fluid total pressure, P_t, was measured in the plenum before entering the 100-hole throat (0.0595 in. in diam) nozzle, a large total pressure loss possibly occurred through the 100-hole throat. The throat was approximately perpendicular to the axes of the divergent portion of the annular-type nozzle (Fig. 5).

The P_{ex}/P_t ratios for the annular-type, ejector-driven diffuser were approximately equal for corresponding driving fluids with the P_{ex}/P_t ratios obtained for the simulated rocket-driven diffuser and are presented in Fig. 7 and Table 1. This P_{ex}/P_t equality was expected from Ref. 1 since the effective L/D for the annular-type, ejector-driven diffuser configuration (L/D = 5.15) was very near the same as for the simulated rocket diffuser configuration (L/D = 6.26). The effect of the contraction due to the centerbody-type ejector and second-throat blockage on P_{ex}/P_t was small.

The annular second-throat diffuser had a physical blockage of 23.25 percent, and the constant area straight diffuser had a physical blockage of 25.54 percent when the centerbody-type ejector was installed. The air performance of the two simulated rocket-driven diffusers in P_{ex}/P_t at start and breakdown was approximately the same as presented in Fig. 7 and Table 1 (P_{ex}/P_t = 0.02050 for constant area straight diffuser with centerbody blockage and P_{ex}/P_t = 0.02152 for the annular second-throat diffuser). Inaccuracies in measurements or the difference in the way blockage was produced resulted in a variation of the P_{ex}/P_t ratios. The larger blockage (25.54 percent) should allow the diffuser to

remain started at a higher exit pressure for a given driving pressure (or higher P_{ex}/P_t) according to Ref. 2.

Figure 8 presents the relationship of P_{ex}/P_t at start and breakdown with respect to the one-dimensional normal shock total pressure ratio from Ref. 6 (P_{ty}/P_{tx}, where x is upstream of normal shock and y is downstream) corresponding to the physical A_d/A^* for the two driving fluids, air and steam. The ratios of the actual P_{ex}/P_t to the one-dimensional normal shock total pressure ratios for the centerbody and annular-type, ejector-driven diffusers are as follows:

Driving Nozzle	A_d/A^*	$(P_{ex}/P_t)_{act} / P_{ty}/P_{tx}$	
		Air	Steam
Centerbody-type	61.03	0.596	0.707
Annular-type	45.92	0.601	0.728

There is little difference in the ratios for $P_{ex}/P_t / P_{ty}/P_{tx}$ for the centerbody and annular-type, ejector-driven diffuser for the corresponding driving fluids. The annular-type ejector has the higher ratios (0.601 for air and 0.728 for steam). The actual physical annular-type ejector nozzle throat area ($A^* = 0.2781$ in.^{2}) was used to get the $A_d/A^* = 45.92$ which in turn gave the P_{ty}/P_{tx} for determining the above ratios. Since the annular nozzle throat was essentially 100 sharp-edge entrance tubes, 0.0595 in. in diameter with length-to-diameter ratio of 7.88, then the effective throat area would be much smaller than the physical area giving a higher A_d/A^*. A higher A_d/A^* would give a lower P_{ty}/P_{tx}. The lower P_{ty}/P_{tx} would increase the $(P_{ex}/P_t)_{act}/(P_{ty}/P_{tx})$. The discharge coefficient for sharp-edge circular orifices in thin plates ranges from 0.56 to 0.79. An approximate average (0.70) of the discharge coefficient range (0.56 to 0.79) was selected. If the effective area of the tubes is assumed to be approximately 0.70 times the physical area (from the 0.70 discharge coefficient), then the effective throat area of the annular nozzle would become $A^* = 0.1947$ in.^{2}, which is approximately equal to the throat area of the centerbody-type ejector nozzle ($A^* = 0.1963$ in.^{2}). This effective annular-type ejector nozzle throat area gives an $A_d/A^* = 65.59$, while the centerbody-type ejector nozzle had an $A_d/A^* = 61.03$. By using the $A_d/A^* = 65.59$ to get P_{ty}/P_{tx}, then the new $(P_{ex}/P_t)_{act}/(P_{ty}/P_{tx})$ ratios for the annular-type, ejector-driven diffuser become 0.849 for air driving fluid and 1.028 for steam. Since the centerbody-type, ejector-driven diffuser installation had a diffuser L/D of 3.70 and the annular-type, ejector-driven diffuser installation had a diffuser L/D of 5.51, then the new ratio $(P_{ex}/P_t)_{act} / (P_{ty}/P_{tx})$

(0.849 for air and 1.028 for steam for the annular-type, ejector-driven diffuser installation is the more nearly correct value as determined from Fig. 10 of Ref. 1 and Fig. 12 of Ref. 3.

4.2 BREAKDOWN PRESSURE RATIO IMPROVEMENT FROM A TANDEM AUXILIARY EJECTOR

Since the purpose of this test was to determine the rocket tailoff characteristics with centerbody-type and annular-type auxiliary ejectors operating in tandem with the rocket, the influence of the ejector on the rocket diffuser performance was pursued. When only the simulated rocket was running (ejector driving pressure, $P_{te} = 0$), a single value of P_{ex}/P_{tr} at breakdown was obtained for each driving gas as presented in Fig. 7 and Table 1. A further improvement in P_{ex}/P_{tr} was obtained by having flow through the auxiliary-type ejector (annular or centerbody). If the auxiliary ejector (annular or centerbody type) was running at some driving pressure, P_{te}, (steam or air), an improvement in P_{ex}/P_{tr} at breakdown resulted. This relationship is presented in Fig. 9 as the ratio of $\frac{(P_{ex}/P_t) \text{ @ } P_{te} > 0}{(P_{ex}/P_t) \text{ @ } P_{te} = 0}$ versus ejector driving pressure-to-rocket driving pressure ratio, P_{te}/P_{tr}, for the simulated rocket driven by air and for the annular-type and centerbody-type ejectors driven by air and steam. The effect of varying the ejector driving pressure, P_{te}, is in effect the same as having a variable second-throat diffuser. The higher P_{te} gives the greater effective second-throat contraction (smaller second-throat duct). There was essentially no difference in the second-throat diffuser performance (P_{ex}/P_t) when the ejector was driven by either air or steam. The data fall on the same line corresponding to the particular type ejector (centerbody or annular) as presented in Fig. 9. The simulated rocket-driven diffuser with the auxiliary annular-type ejector remains started at a much higher P_{ex}/P_{tr} ratio (or higher P_{ex} for a given P_{tr}) than will the rocket-driven diffuser with the auxiliary centerbody-type ejector. This higher P_{ex}/P_{tr} ratio obtained for the rocket-driven diffuser with the annular-type ejector means that the annular-type ejector gives a greater effective second-throat contraction than does the centerbody-type ejector for a given ejector driving pressure. The auxiliary tandem ejector (centerbody or annular type) aids the simulated rocket diffuser-ejector performance only by increasing the operating range of P_{ex}/P_t in the form of an effective variable area second throat.

The auxiliary tandem ejector has an additional function during simulated rocket ignition and tailoff. This function is to hold the proper altitude during the ignition and the tailoff phases of the rocket firing. Holding

a constant altitude (cell pressure, P_c) during the simulated ignition and tailoff phases with the auxiliary ejector is impossible since the rocket chamber pressure, P_{tr}, controls P_c when P_{ex} is sufficiently low for the diffuser to be started at the particular ejector driving pressure. On tailoff, since P_c is controlled directly by P_{tr} until breakdown, P_c decreases directly with decreasing P_{tr} until P_{tr} becomes too low to buck the relative constant P_{ex}. After this low P_{tr} limit is reached, the rocket diffuser-ejector pumping action breaks down, which causes P_c to increase as a result of the high pressure jet stream rushing back into the test cell before the auxiliary ejector can pump from the diffuser the volume of mass in the region between the rocket nozzle exit and the ejector nozzle exit (pumping secondary flow). A small quantity of secondary flow will increase P_c tremendously from the no secondary flow P_c value. Secondary flow on the order of one percent of the jet pump driving fluid flow will cause P_c to increase to a value approximately 4 times the P_c at no secondary flow.

4.3 STEPWISE STEADY-STATE SIMULATED ROCKET TAILOFF WITH TANDEM AUXILIARY ANNULAR-TYPE EJECTOR

Presented in Fig. 10 is a typical rocket tailoff with the annular-type auxiliary ejector. The exit pressure was held relatively constant, while the rocket chamber pressure was decreased in steps until and after breakdown. Simulated rocket tailoff data were obtained while the ejector driving pressure was held constant at two different values (P_{te} = 209 and 151 psia for air driving fluid) to determine the effect of ejector driving pressure on the diffuser breakdown pressure ratio, P_{tr}/P_{ex}. The performance of the rocket driven diffuser-ejector both with a constant area straight diffuser (Fig. 4) and with the annular second-throat diffuser (Fig. 5) (installation Figs. 2a and c) is presented in Fig. 10. The data fall on a single line except after breakdown. This figure presents the improvement in performance obtained by first adding a physical second throat with contraction area ratio of A_{st}/A_d = 0.7665 to the constant area straight diffuser and then decreasing the effective A_{st}/A_d by driving the annular-type ejector with P_{te} = 151 and 209 psia. The improvement in P_{tr}/P_{ex} at breakdown is as follows:

Diffuser	Ejector Driving Pressure, P_{te}	P_{tr}/P_{ex} at Breakdown
Constant area straight diffuser	No ejector installed	54.64
Second-throat diffuser only	Ejector not running	46.46
Second-throat diffuser and annular-type ejector	151	28.10
Second-throat diffuser and annular-type ejector	209	22.50

The straight portion of the curve indicates the direct variation of P_c with P_{tr} as long as the diffuser is started. As P_{tr} decreased lower than the breakdown rocket driving pressure but before it reached zero for the set exit pressure, the cell pressure increased to a point a little higher than the value obtained when the rocket driving pressure was zero (ejector only running). After rocket breakdown, the remaining flow of the rocket until P_{tr} reached zero was secondary flow to the annular-type ejector. This secondary flow allowed P_c to increase higher than the zero secondary flow P_c of the ejector. As the secondary flow was decreased (pumped out of the cell by the ejector), P_c decreased to the ejector zero secondary flow P_c corresponding to the cell-to-ejector driving pressure ratio, P_c/P_{te}, in Fig. 7.

When steam was used as the ejector driving fluid, the test cell pressure data should have been in line with the air data since the rocket was driven by air. However, steam ejector data were much higher than the air ejector data. Since the steam was a two-phase fluid (very wet) after the expansion through the nozzle and since the rocket was not running when the annular-type ejector driving fluid was first increased, condensation was forced into the test cell -- especially when the annular ejector breakdown was determined. Evaporation of the condensate limited the cell pressure when the rocket was started. If the rocket had been running before the ejector was started, the steam could not have reached the test cell, and, thus, the steam ejector data might have been in line with the air ejector data. The breakdown point is also lower than it should be as obtained from Fig. 9.

4.4 STEPWISE STEADY-STATE SIMULATED ROCKET TAILOFF WITH TANDEM AUXILIARY CENTERBODY-TYPE EJECTOR

Rocket tailoff data were taken for the centerbody-type ejector configuration (Fig. 2b) and are presented in Fig. 11 along with the rocket and annular-type ejector air performance curve from Fig. 10. The performance of the constant area straight diffuser without the centerbody-type ejector, the constant area straight diffuser with the centerbody-type ejector, and the constant area straight diffuser with the centerbody-type ejector operating at various driving pressures is presented in Fig. 11. When the rocket was running without the ejector running, the data fall on the rocket and annular-type ejector performance line from Fig. 10.

Again the variable second-throat effect is evident by first installing the centerbody-type ejector in the constant area straight diffuser and then running the ejector with various driving pressures. The higher ejector driving pressure results in a greater effective contraction which gives the lower P_{tr}/P_{ex} (allows the diffuser to operate at a higher exit

pressure). The dashed, almost vertical, lines indicate breakdown. Unlike the steam-driven, annular-type ejector data presented in Fig. 10, the steam-driven, centerbody-type ejector data fall in line with the air-driven, centerbody-type ejector data (Fig. 11). Both the air and steam-driven, centerbody-type ejector test cell data were higher than were the air-driven rocket performance data when the ejector was not running. A possible explanation for this difference in performance is that condensation could have gotten into the test cell from the manner in which the rocket and ejector were run. The air-driven rocket driving pressure was varied through breakdown, while the steam-driven centerbody-type ejector driving pressure remained constant. During this time of diffuser breakdown, condensation was allowed to collect in the test cell. This is evident from the decrease in the ejector driving pressure, P_{te}, to 100 psia. The data moved closer to the annular ejector data line.

From this stepwise rocket tailoff, data for P_{te} = 244 psia after breakdown indicate that P_c increased rapidly to a value much higher than that which the ejector alone gives for the P_{te} = 244 psia. The P_c calculated from Fig. 7 for the P_{te} = 244 psia is 0.122 psia, which gives P_c/P_{ex} = 0.03675. This point is plotted in Fig. 11 for P_{tr} = 0 (rocket not running).

The rocket was driven by steam to simulate hot rocket gas, and the centerbody-type ejector was driven by air at different pressure levels, P_{te}, during stepwise rocket tailoff. This rocket tailoff performance is presented in Fig. 12. The trend of the performance with a steam-driven rocket and air-driven ejector is similar to that obtained with the air-driven rocket and an air and steam-driven ejector as shown in Figs. 10 and 11, respectively. The data follow a straight line as long as the diffuser remains started. As the ejector driving pressure is increased, giving a greater effective second-throat contraction, the operating range of the diffuser is increased by decreasing P_{tr}/P_{ex} (allowing the diffuser to operate at a higher exit pressure). Unlike the air-driven rocket performance, the steam-driven rocket performance at breakdown was an instantaneous cell pressure increase to approximately 10 times that before breakdown. When the rocket pressure, P_{tr}, was reduced to zero, approximately 5 minutes were required after diffuser breakdown before the ejector could pump the cell pressure to the level corresponding to the driving pressure, P_{te}, obtained from the performance presented in Fig. 7. This high cell pressure peak and the time period required to pump the proper cell pressure after breakdown were a result of condensation (from the steam-driven rocket) in the test cell after breakdown.

The slope of the started portion of the steam-driven rocket, air-driven ejector tailoff curve is different from that of the steam-driven

rocket performance presented in Figs. 7 and 12. The rocket-driven diffuser performance in Fig. 7 was obtained at a constant driving pressure, P_{tr} = 190 psia, and represents the constant P_c/P_t relationship of 0.0015, whereas in Fig. 12 the rocket pressure was decreased to breakdown and then to zero for various ejector driving pressures. The total temperature, T_{tr}, of the steam driving fluid decreased approximately 100°F as the driving pressure, P_{tr}, decreased toward breakdown. This decrease in temperature caused the P_c/P_{tr} (or P_c/P_{ex}, where P_{ex} is constant, to be high) ratio to increase by approximately 80 percent as a result of the expansion of an increasingly wetter fluid (two-phase fluid expansion). Saturated expansion phenomenon is discussed in more detail in Ref. 7.

4.5 TRANSIENT SIMULATED ROCKET TAILOFF WITH TANDEM AUXILIARY CENTERBODY-TYPE EJECTOR

The rocket tailoff data previously discussed and presented in Figs. 10, 11, and 12 were for a simulated rocket tailoff through stepwise steady-state decrease in rocket driving pressure at various ejector driving pressures with the diffuser exit pressure held constant near diffuser breakdown when only the rocket was driving the diffuser. A more nearly simulated rocket tailoff study was made for an air-driven rocket and steam-driven ejector by continuously decreasing the rocket driving pressure to zero while the cell, rocket, ejector, and diffuser exit pressures were recorded on null-balance, potentiometer-type, strip-chart recorders. A typical transient of rocket pressure, P_{tr}, is presented in Fig. 13. The P_{tr} was decreased from approximately 300 psia to 0 in approximately 12 sec. The simulated rocket tailoff transients were made for various ejector driving pressures both with diffuser exit pressure sufficiently low so that the ejector was started when the rocket was off (P_{tr} = 0) and with P_{ex} high enough so that the ejector was not started when the rocket was off. Figure 14 presents these transient data both for rocket tailoff and ignition.

The various ejector driving pressures produced the variable effective second-throat in the same manner as was found in the stepwise steady-state data presented in Figs. 10, 11, and 12. The stepwise steady-state data are in good agreement with the transient data as presented in Fig. 14; this indicates apparently no time lag. The diffuser breakdown was in agreement with the breakdown determined from Fig. 9 for the various ejector driving pressures. The breakdown pressure ratio, P_{tr}/P_{ex}, was set by the ejector driving pressure, fixing the effective second-throat area. If the ejector driving pressure was sufficiently high for starting the diffuser for the particular exit pressure,

the cell pressure peaked at a value approximately four times the P_c before diffuser breakdown as P_{tr} was decreased to zero. The P_c peak was in no case eliminated even if the diffuser exit pressure was much lower than that required at breakdown during the transient rocket tailoff. The P_c peak is a characteristic result of an auxiliary ejector changing from a jet pump (pump secondary flow) after breakdown but before the rocket chamber pressure reaches zero to a diffuser-ejector (pumps no secondary flow) when the rocket chamber pressure is zero. The peak may be damped by having the auxiliary ejector just as close to the nozzle exit as possible without affecting cell pressure so that the volume between the rocket and ejector is a minimum.

The ignition portion of the curve (P_{tr} increased from zero) in Fig. 14 is similar to the tailoff portion. The diffuser start and breakdown pressure ratios, P_{tr}/P_{ex}, are essentially the same for the corresponding ejector driving pressure. During ignition (as in tailoff) the cell pressure first increased and then decreased as the rocket driving pressure increased before the diffuser started.

4.6 COMPARISON OF THE ANNUAL-TYPE AND CENTERBODY-TYPE EJECTOR PERFORMANCE

The annular-type ejector appears to give better performance than the centerbody-type. The rocket and annular-type ejector tailoff performance curve presented in Fig. 10 is shown as a dashed line in Fig. 14. The cell pressure peak for the rocket and annular-type ejector performance is not as high as that obtained with the centerbody-type ejector. The breakdown pressure ratio, P_{tr}/P_{ex}, was lower for the same ejector driving pressure for the annular-type ejector than it was for the centerbody-type ejector.

The apparent advantage of the annular-type ejector over the centerbody-type ejector is that there is no obstruction in the center of the diffuser such as the centerbody that produces shock systems (high losses) in the high velocity jet stream from the rocket nozzle which may be supersonic, sonic, or high subsonic even after the pumping action of the rocket-driven diffuser has broken down. Since there is no bow shock in the high velocity region (centerline of diffuser), the trailing mass from the rocket in the annular-type ejector configuration has less energy loss than the centerbody-type ejector; therefore, the trailing mass reaches the ejector jet stream for entrainment at a high energy level. The ejector jet stream imparts additional energy to the slower moving molecules of the rocket trailing mass. This higher mass-energy level for the annular-type ejector prevents the test cell pressure from reaching

the high peak that is normally reached after diffuser breakdown for the centerbody-type ejector. It appears that improvement on the design of the annular-type ejector can greatly improve the performance in the transition region during rocket tailoff. A continuous annular smooth approach to and from the throat in line with the flow will drastically reduce the pressure losses through the nozzle and will result in better nozzle performance.

The design of the annular-type ejector used in this investigation (Fig. 6) and the first of the two sketches shown below could be greatly improved by going to a design similar to the second sketch shown.

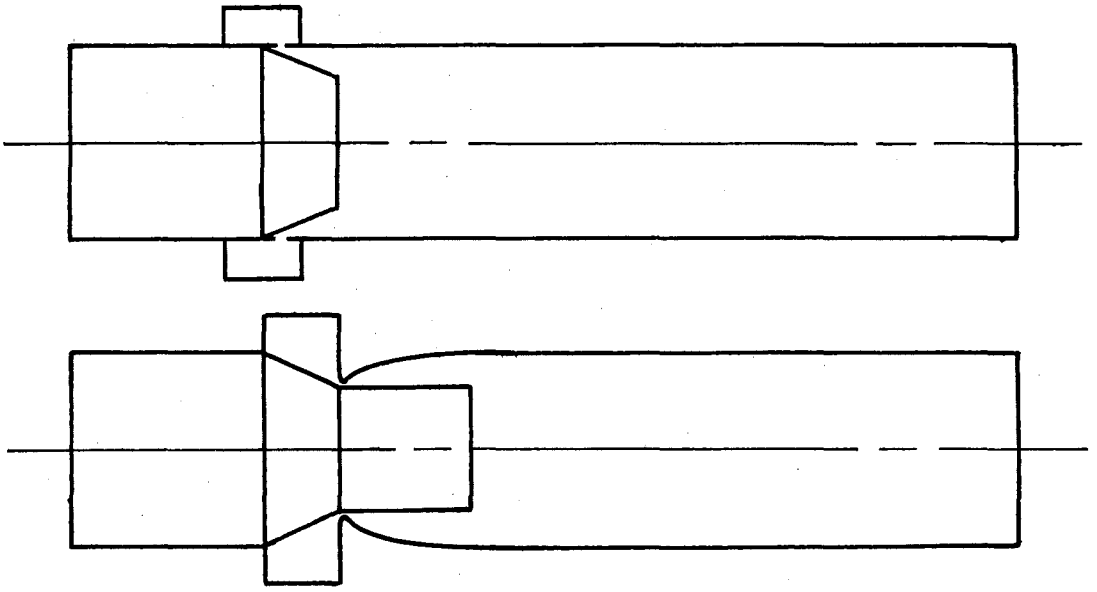

This design would have essentially parallel exit flow from the annular nozzle exit. Reference 4 indicates that the no-secondary-flow P_c/P_t ratio, which a parallel exit flow nozzle ($\theta_n = 0$) can pump in a diffuser, is much lower than that ratio, P_c/P_t, which a conical nozzle can pump for the same A_d/A^* (on the order of 1/3 of the conical nozzle P_c/P_t for $\theta_n = 18°$). If this improvement could be realized in an annular-type, ejector-driven diffuser for parallel exit flow (design shown above), then based on the no-secondary-flow performance for the annular-type ejector presented in Fig. 10, the improvement would bring the no-secondary-flow, annular-type, ejector-driven diffuser performance in line with the centerbody-type, ejector-driven diffuser performance. According to unpublished data preliminary investigations indicate that a small quantity of secondary flow will increase the P_c/P_t ratio performance of a diffuser driven by a small half-angle (θ_n) nozzle more than it does a diffuser driven by a large half-angle nozzle [(P_c/P_t without secondary flow)/(P_c/P_t with secondary flow) ratio is lower for nozzles with small half angles, θ_n]. This loss in performance may cause the

difference between the peak cell pressure on rocket tailoff and the no-secondary-flow cell pressure ($P_{tr} = 0$) to be higher than that experienced in rocket tailoff with the annular-type ejector performance presented in Fig. 10, but the peak cell pressure is not expected to be as high as it was for the annular-type ejector investigation.

5.0 SUMMARY OF RESULTS

The results of the model study of rocket tailoff with auxiliary (centerbody or annular-type) ejector are summarized as follows:

1. The auxiliary tandem ejector (centerbody or annular-type regardless of type of driving fluid) aids the air-driven rocket diffuser-ejector performance by increasing the diffuser exit-to-total pressure ratio, P_{ex}/P_t, operating range. This increase is made possible by varying the ejector air or steam driving pressure which changes the effective second-throat contraction ratio, A_{st}/A_d, and thus provides an effective variable area second throat.
2. The annular-type auxiliary ejector allows the rocket-driven diffuser to remain started at a diffuser exit-to-total pressure ratio, P_{ex}/P_t, as high as 1.50 times the P_{ex}/P_t ratio allowed by the centerbody-type auxiliary ejector when driven by the same ejector driving pressure, P_{te}. This higher P_{ex}/P_t ratio before diffuser breakdown obtained with the tandem air or stream driven annular-type ejector over the tandem air or steam driven centerbody-type ejector resulted from the apparently greater effective second-throat contraction (A_{st}/A_d smaller) produced by the annular-type over the centerbody-type ejector.
3. A decrease of as much as 100°F in steam driving fluid temperature as the driving pressure was decreased for rocket tailoff resulted in an increase in cell-to-rocket chamber pressure ratio, P_c/P_{tr}, of approximately 80 percent. This performance is characteristic of the expansion of an increasingly wetter driving fluid (two-phase fluid expansion).

REFERENCES

1. Hale, James W. "Investigation of Two-Nozzle Cluster Diffuser-Ejector with and without Ejected Mass." AEDC-TDR- (To be published).

2. Bauer, R. C. and German, R. C. "The Effect of Second-Throat Geometry on the Performance of Ejectors without Induced Flow." AEDC-TN-61-133, November 1961.

3. Barton, D. L. and Taylor, D. "An Investigation of Ejectors without Induced Flow." AEDC-TN-59-145, December 1959.

4. Latvala, E. K. "Spreading of Rocket Exhaust Jets at High Altitudes." AEDC-TR-59-11, June 1959.

5. German, R. C. and Bauer, R. C. "Effects of Diffuser Length on the Performance of Ejectors without Induced Flow." AEDC-TN-61-89, August 1961.

6. Wang, C. J., Peterson, J. B., and Anderson, R. "Gas Flow Tables." GM-TR-154, March 1957.

7. Hale, James W. "Comparison of Diffuser-Ejector Performance with Five Different Driving Fluids." AEDC-TDR- (To be published).

TABLE 1

SUMMARY OF TEST DATA

I. Air Driving Fluid

INSTALLATION	P_{ex}/P_t at Breakdown	P_c/P_t
Rocket-driven diffuser with centerbody-type ejector installed . .	0.02050	0.00055
Rocket-driven diffuser with no centerbody-type ejector installed . .	0.01830	0.00055
Rocket-driven, second-throat, annular-type ejector diffuser	0.02152	0.00060
Centerbody-type, ejector-driven diffuser	0.01550	0.00050
Annular-type, ejector-driven, second-throat diffuser	0.02050	0.00255

II. Steam Driving Fluid

INSTALLATION		
Rocket-driven diffuser with centerbody-type ejector installed	0.02550	0.00150
Centerbody-type, ejector-driven diffuser	0.01950	0.00150
Annular-type, ejector-driven, second-throat diffuser	0.02630	0.00500

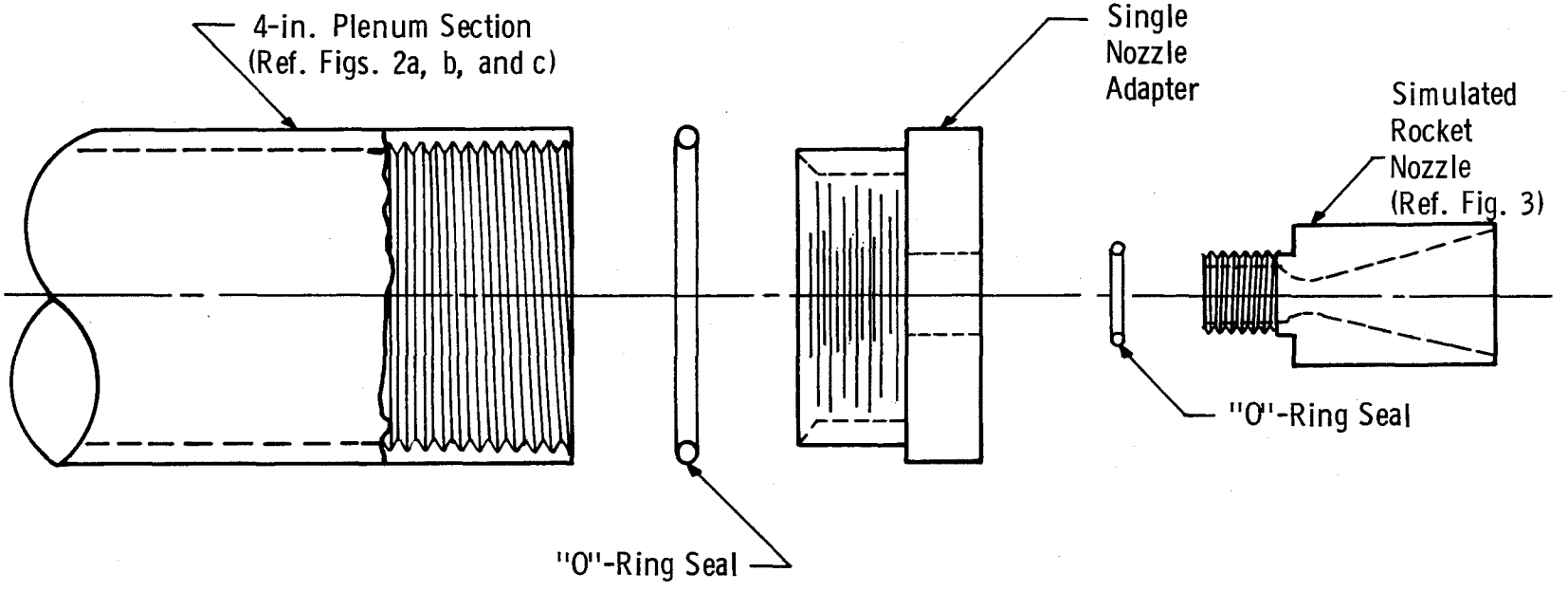

Fig. 1 Simulated Rocket Nozzle Assembly with Plenum Section and Adapter

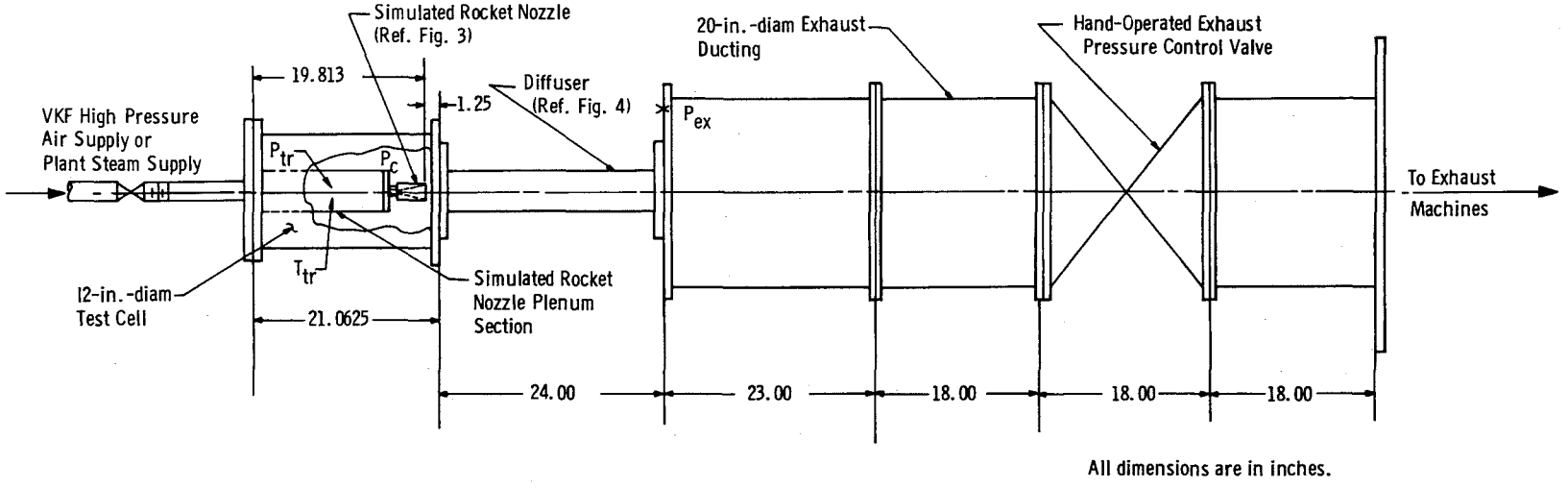

a. Constant Area Straight 4.032-in. Diffuser

Fig. 2 T-5BR1 Test Installation

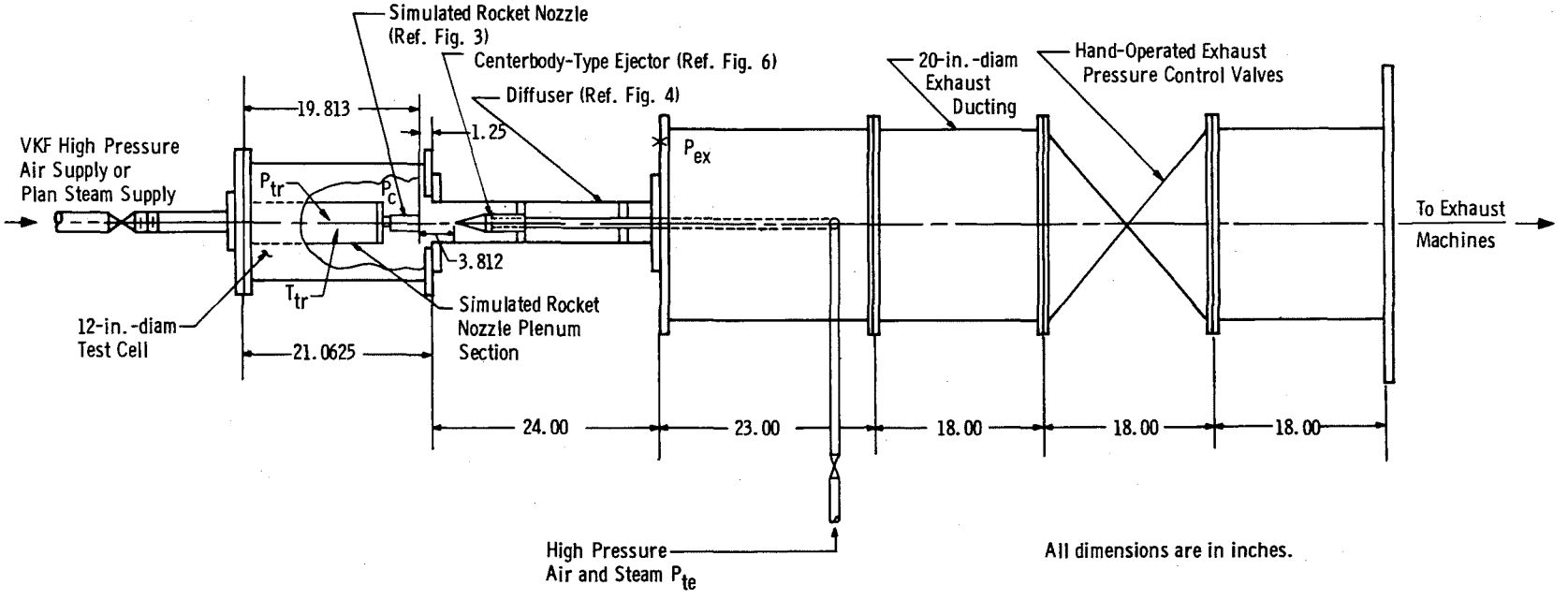

b. Constant Area Straight 4.032-in. Diffuser with Centerbody-Type Auxiliary Ejector

Fig. 2 Continued

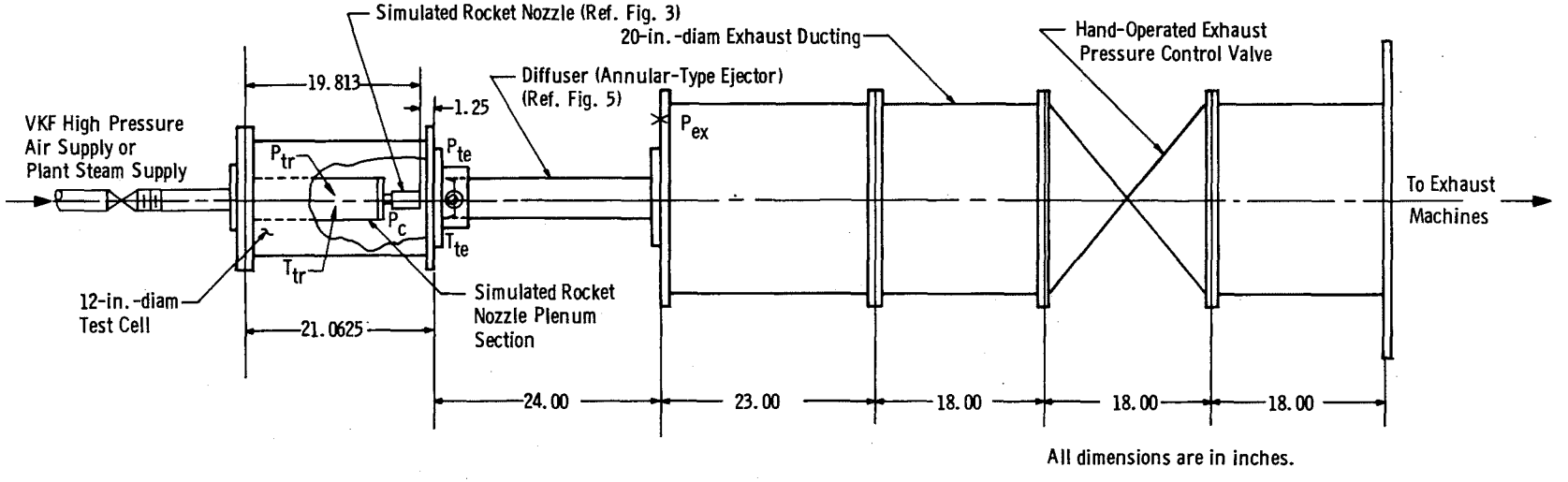

c. Second-Throat Diffuser with Annular-Type Auxiliary Ejector

Fig. 2 Concluded

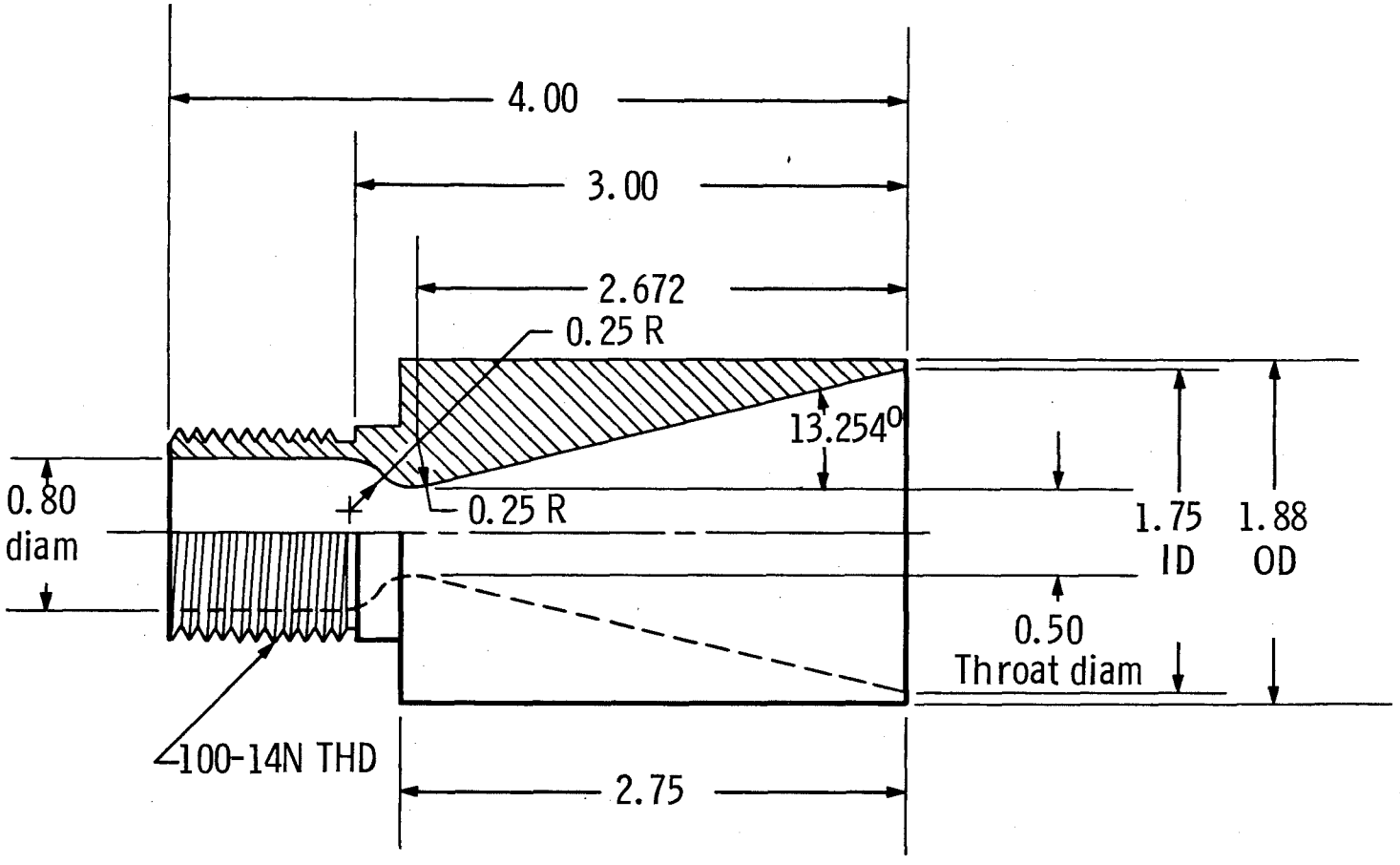

Fig. 3 Simulated Rocket Nozzle Details

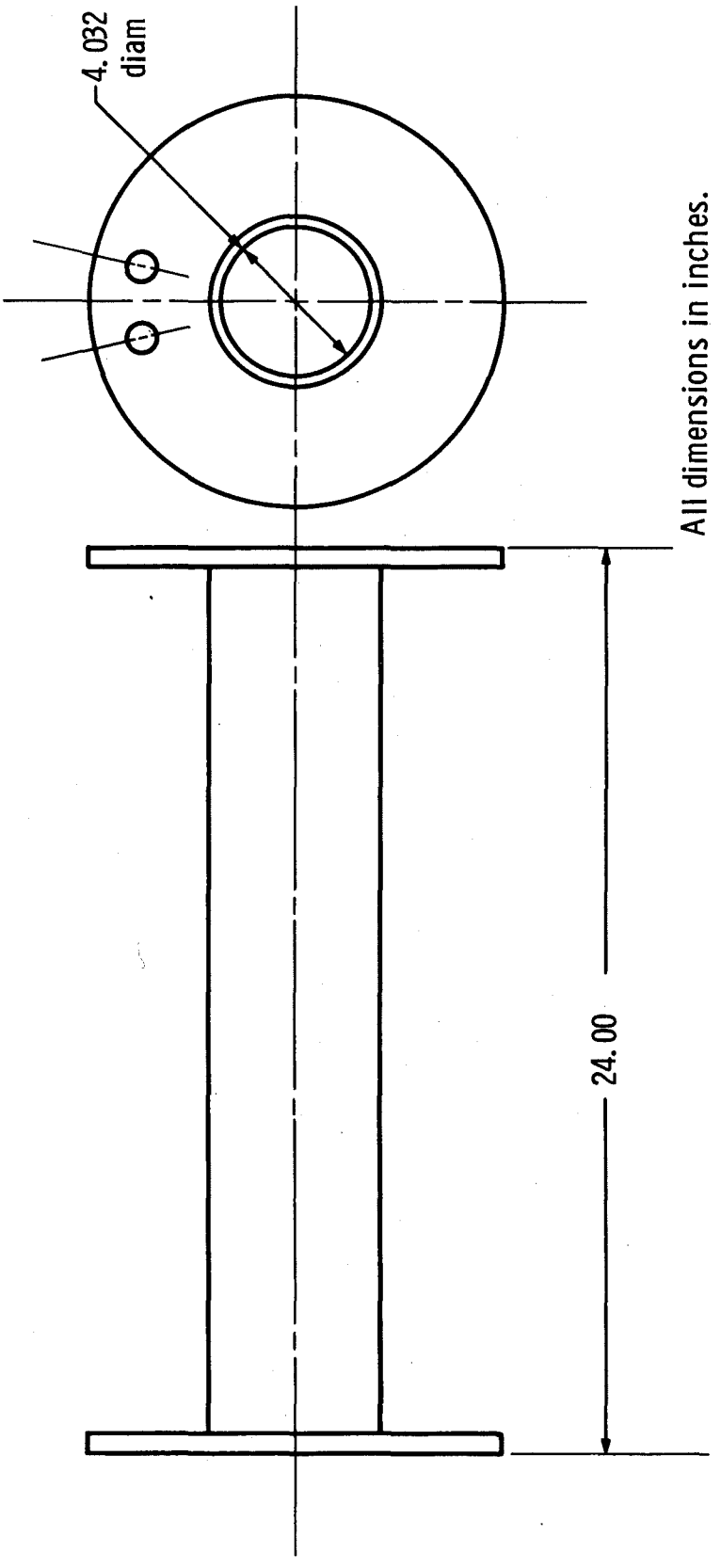

Fig. 4 Constant Area Straight 4.032-in. Diffuser Details

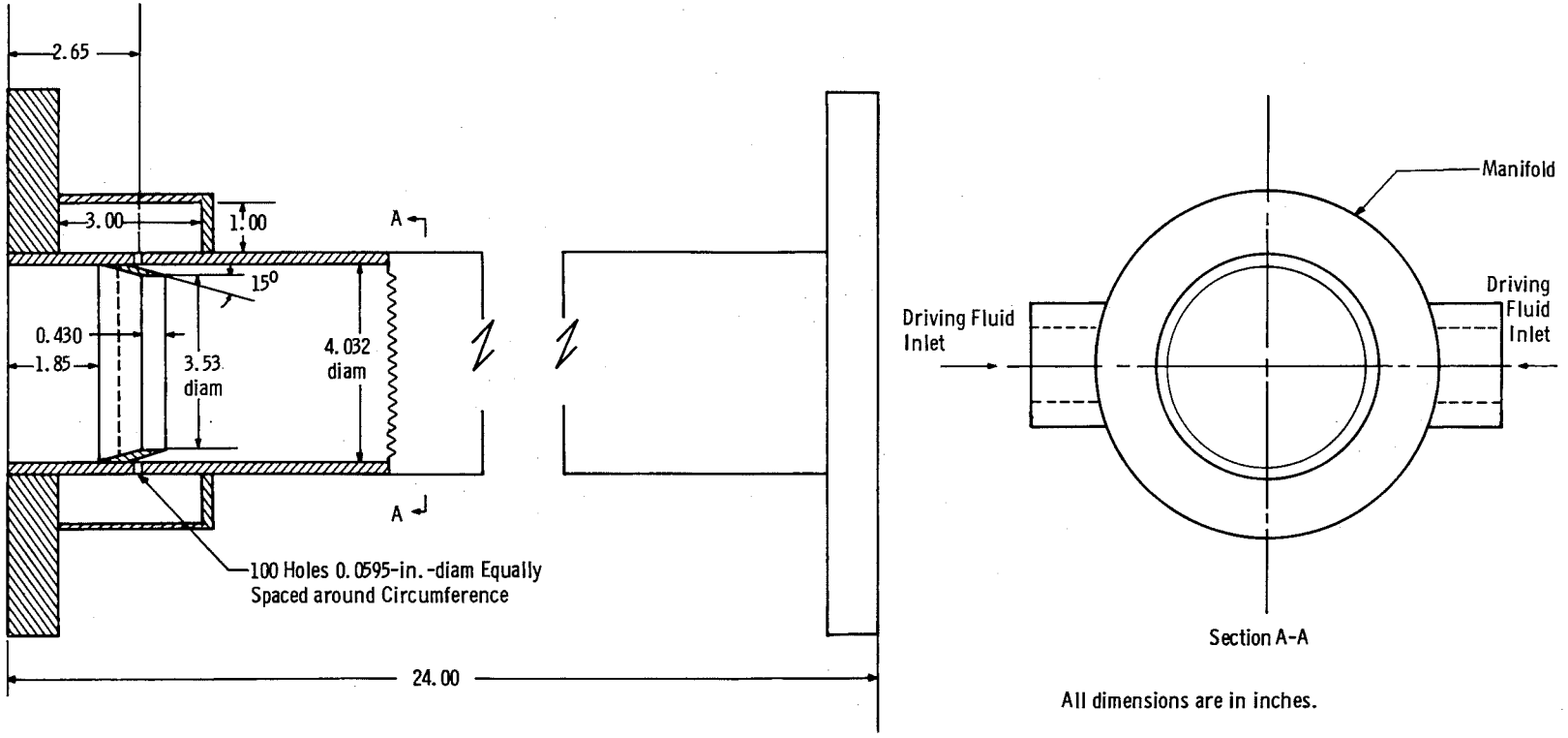

Fig. 5 Second-Throat Diffuser with Annular-Type Auxiliary Ejector Details

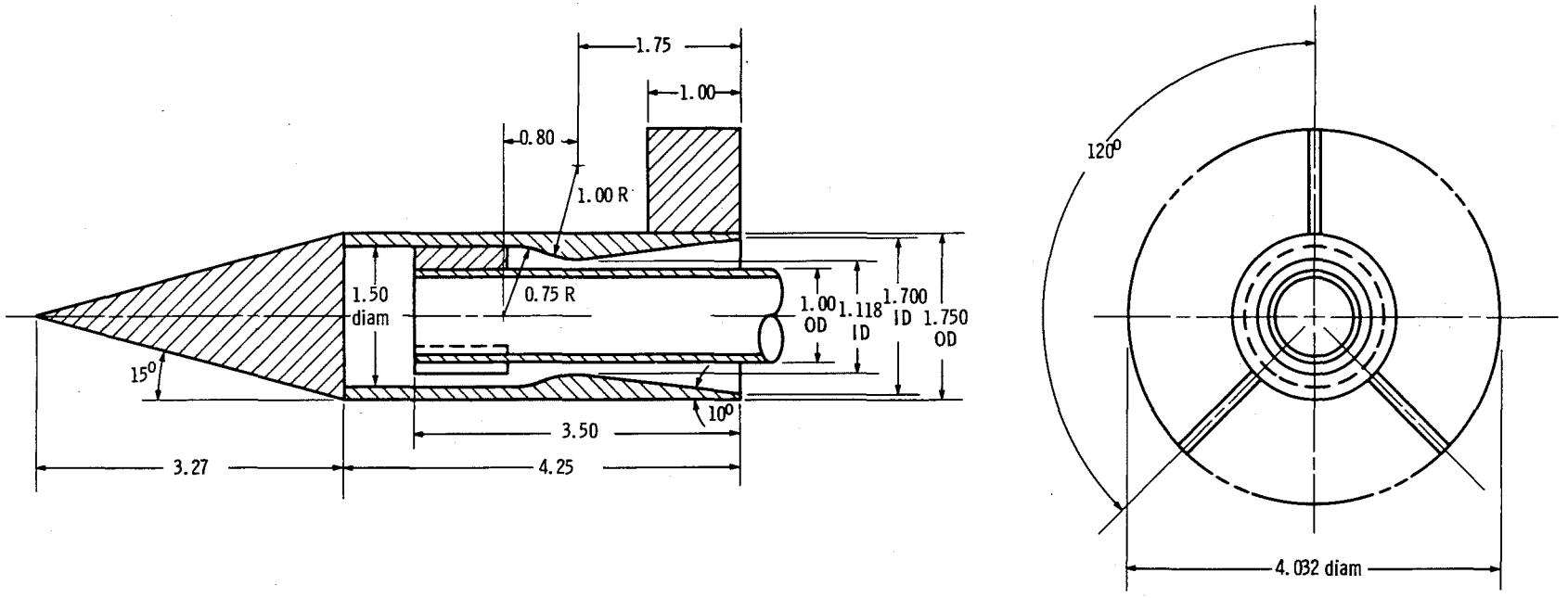

All dimensions are in inches.

Fig. 6 Centerbody-Type Auxiliary Ejector Details

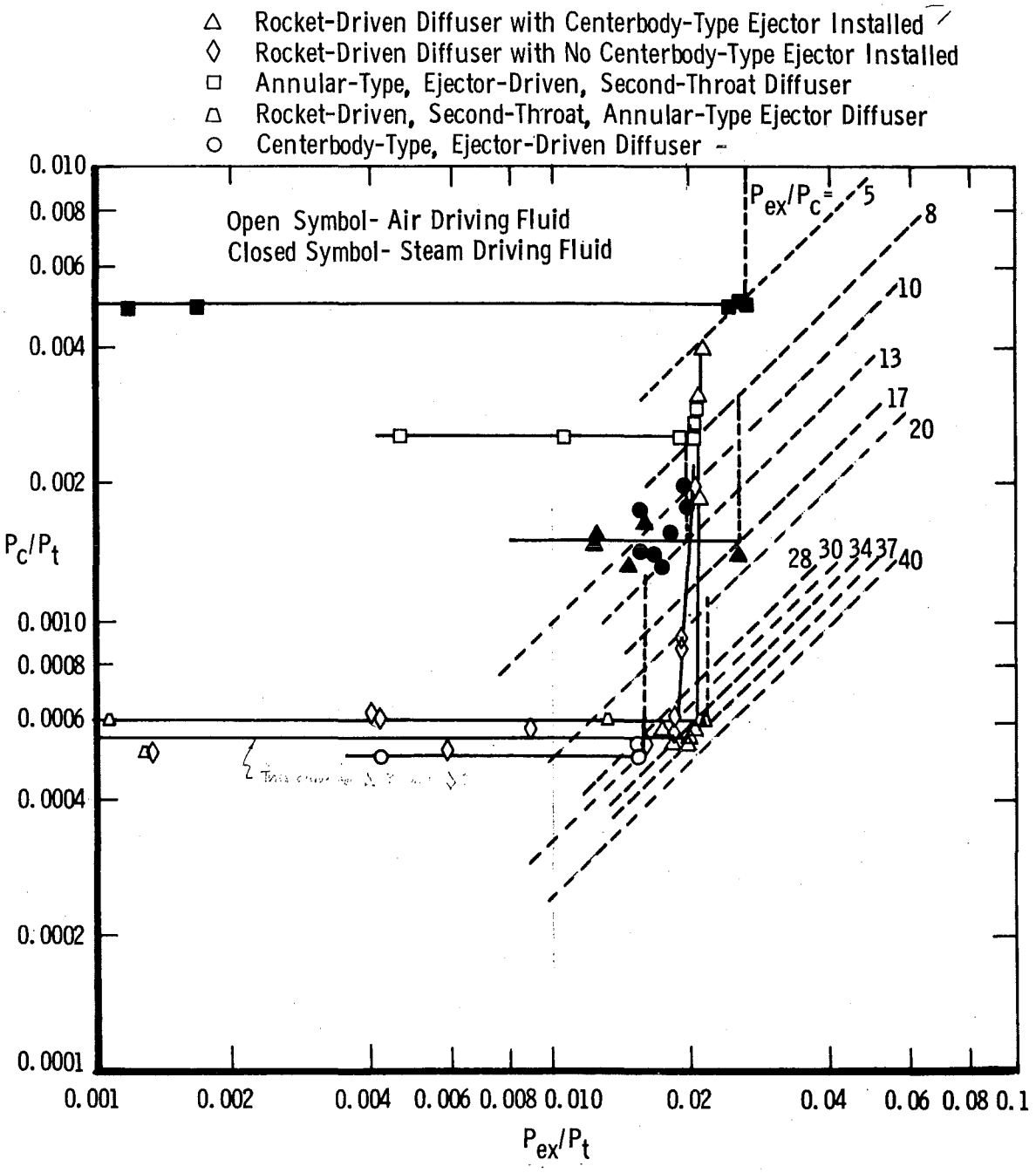

Fig. 7 Performance of Individual-Rocket-Driven and Auxiliary-Ejector-Driven, Diffuser-Ejector Configurations

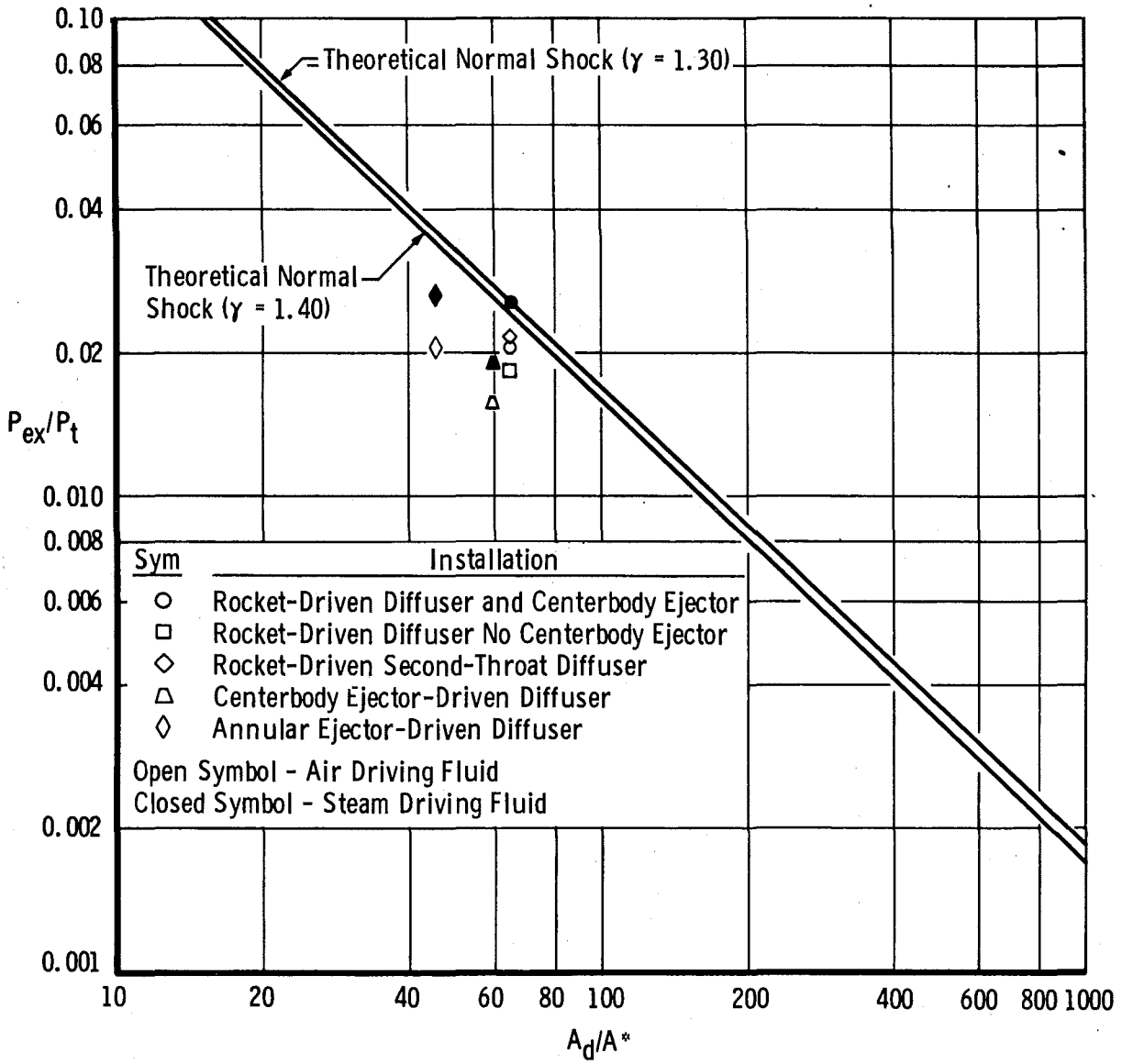

Fig. 8 Diffuser-Ejector Average Pressure Ratio Required for Starting

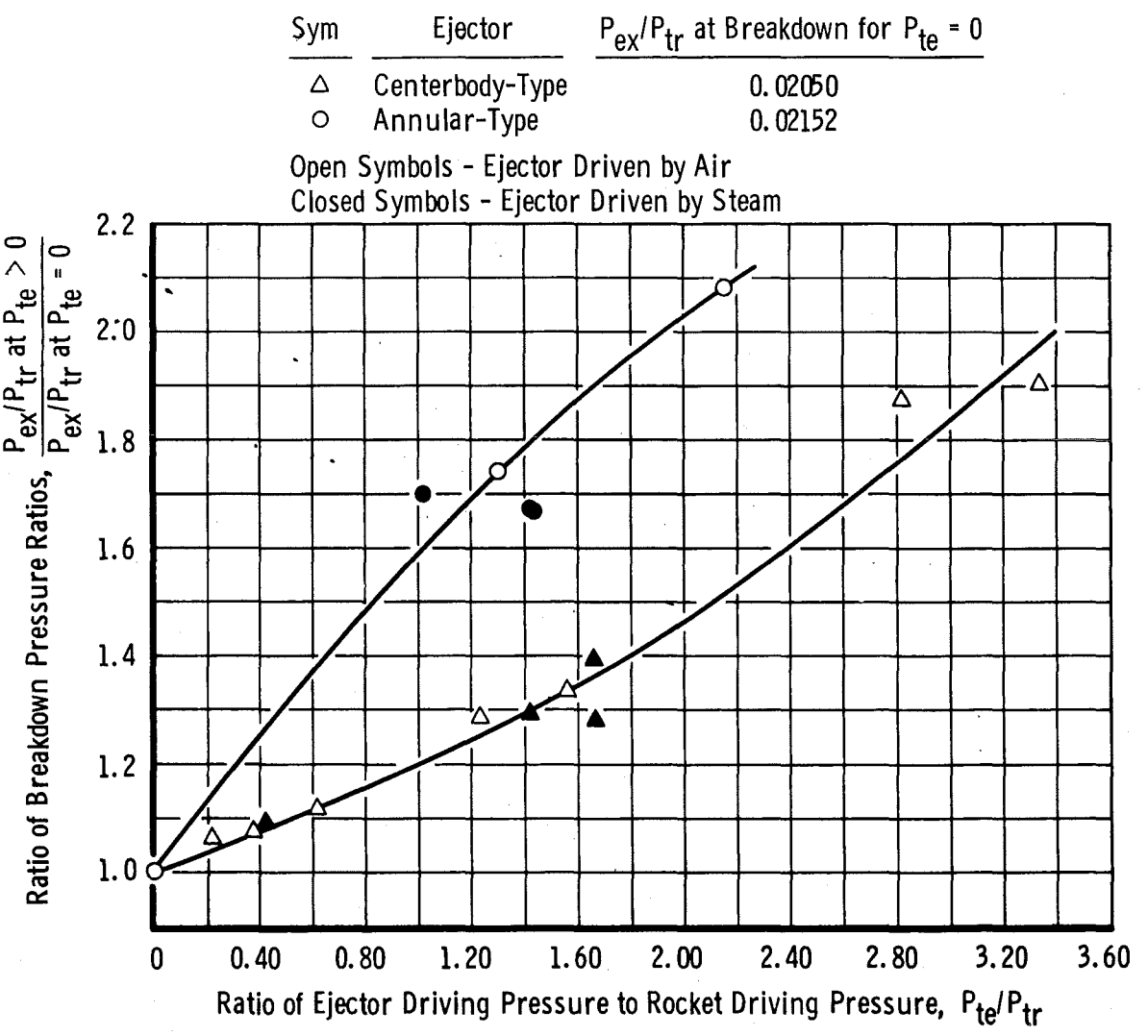

Fig. 9 Air-Driven-Rocket, Diffuser-Ejector Breakdown Pressure Ratio Improvement with Increasing Ejector Driving Pressure

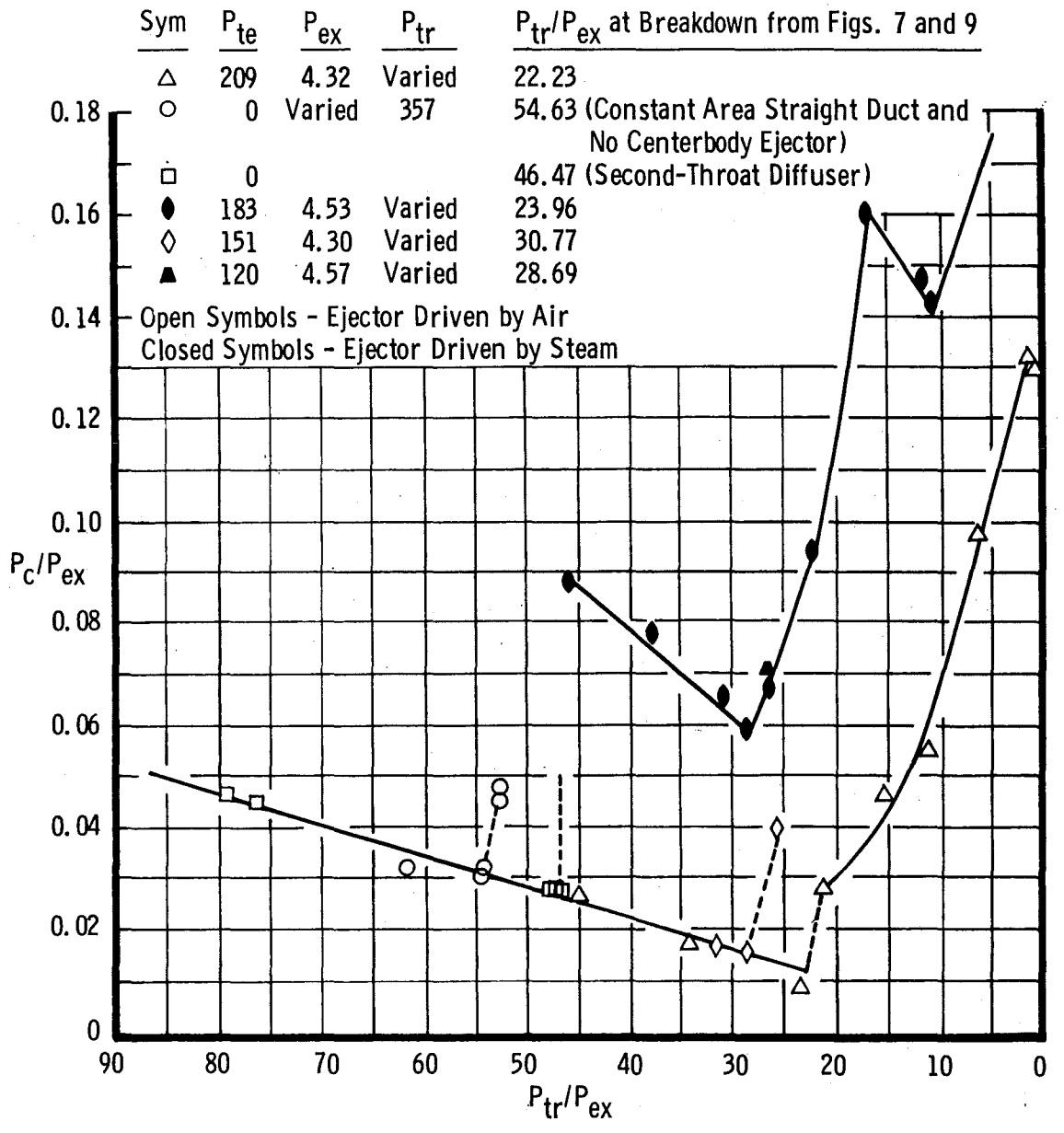

Fig. 10 Air-Driven-Rocket, Stepwise Steady-State Tailoff with Auxiliary Annular-Type Ejector

Sym	P_{te}	P_{ex}	P_{tr}	P_{tr}/P_{ex} at Breakdown from Figs. 7 and 9
○	274	3.40	Varied	24.89
△	200	3.40	Varied	34.54
□	100	3.47	Varied	43.36
◇	162	3.43	131	38.41
◊	244	3.32	Varied	28.86
♦	190	3.20	Varied	36.01
D	0	Varied	357	54.64 (Constant Area Straight Diffuser and No Centerbody Ejector)
⏢	0	Varied	410	48.78 (Straight Diffuser with Centerbody Ejector)

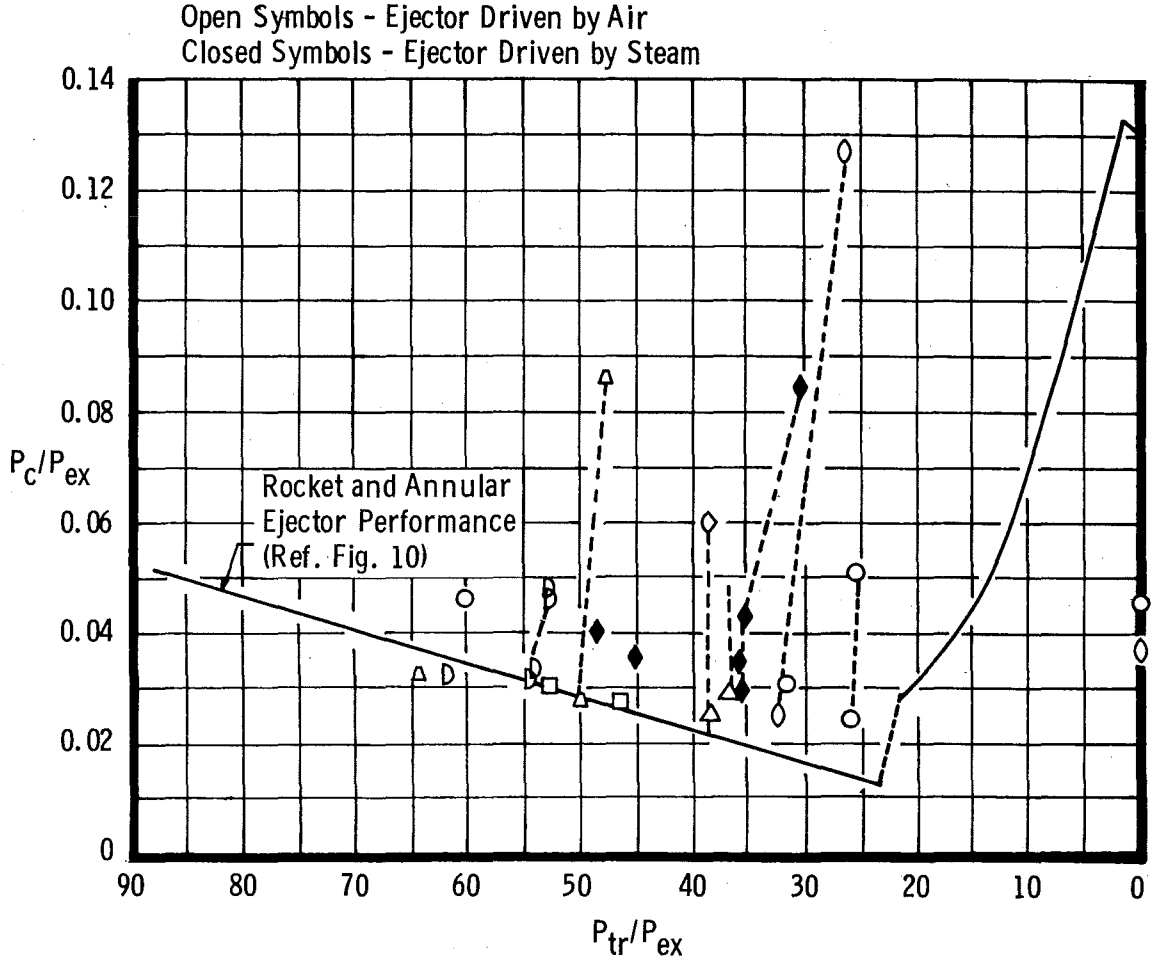

Fig. 11 Air-Driven-Rocket, Stepwise Steady-State Tailoff with Auxiliary Centerbody-Type Ejector

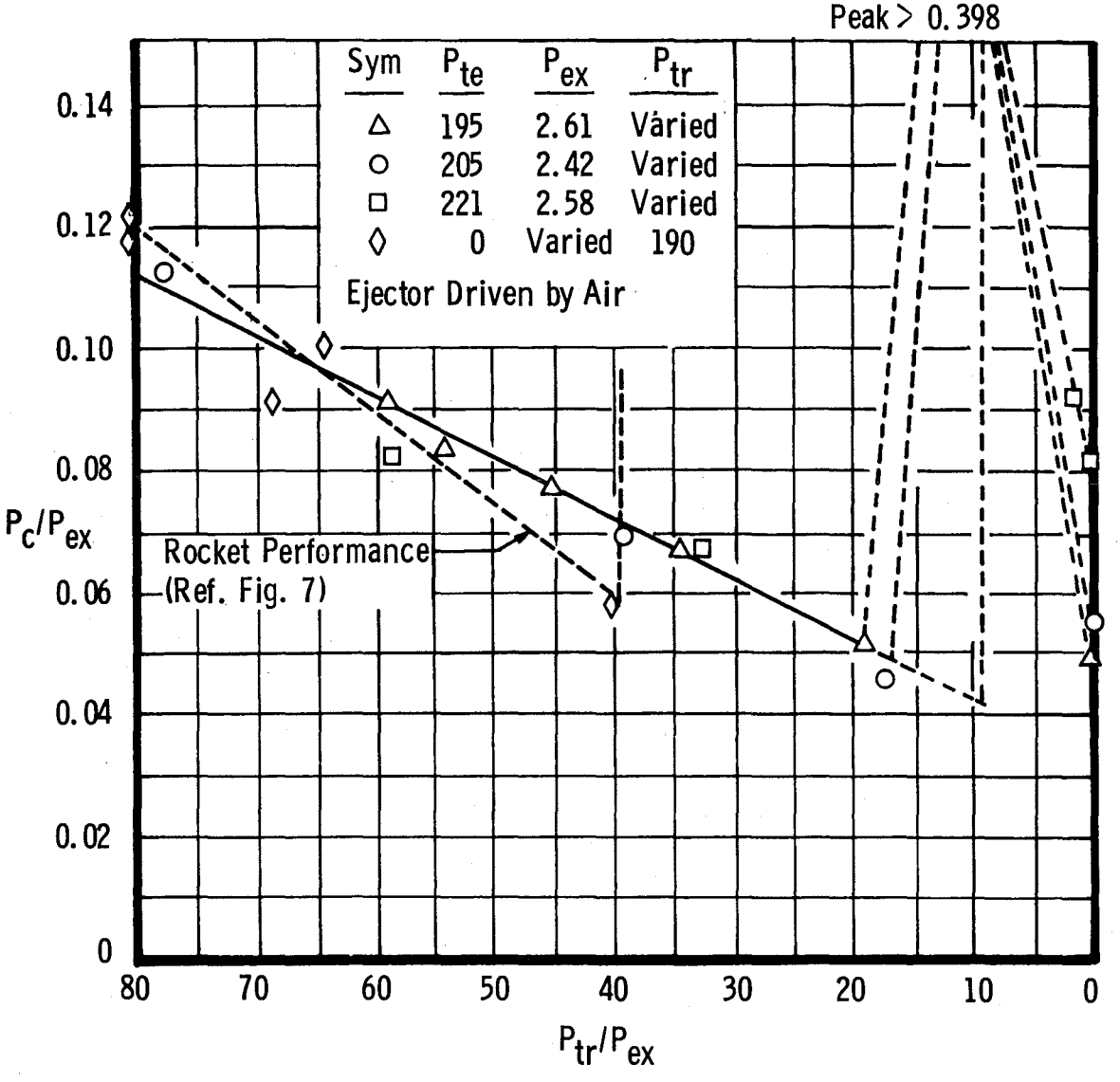

Fig. 12 Stream-Driven-Rocket, Stepwise Steady-State Tailoff with Auxiliary Centerbody-Type Ejector

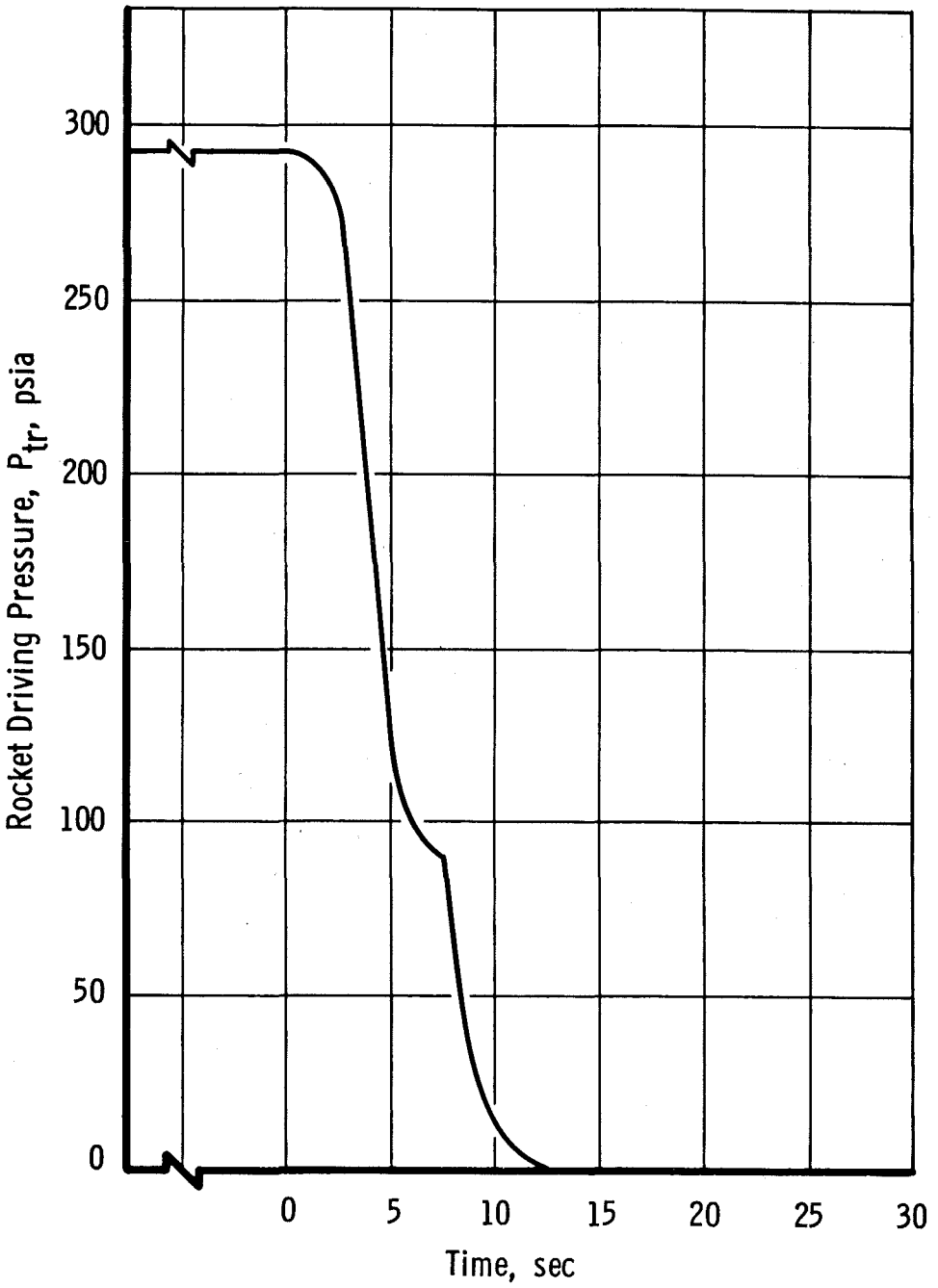

Fig. 13 Typical Transient of Rocket Pressure, P_{tr}

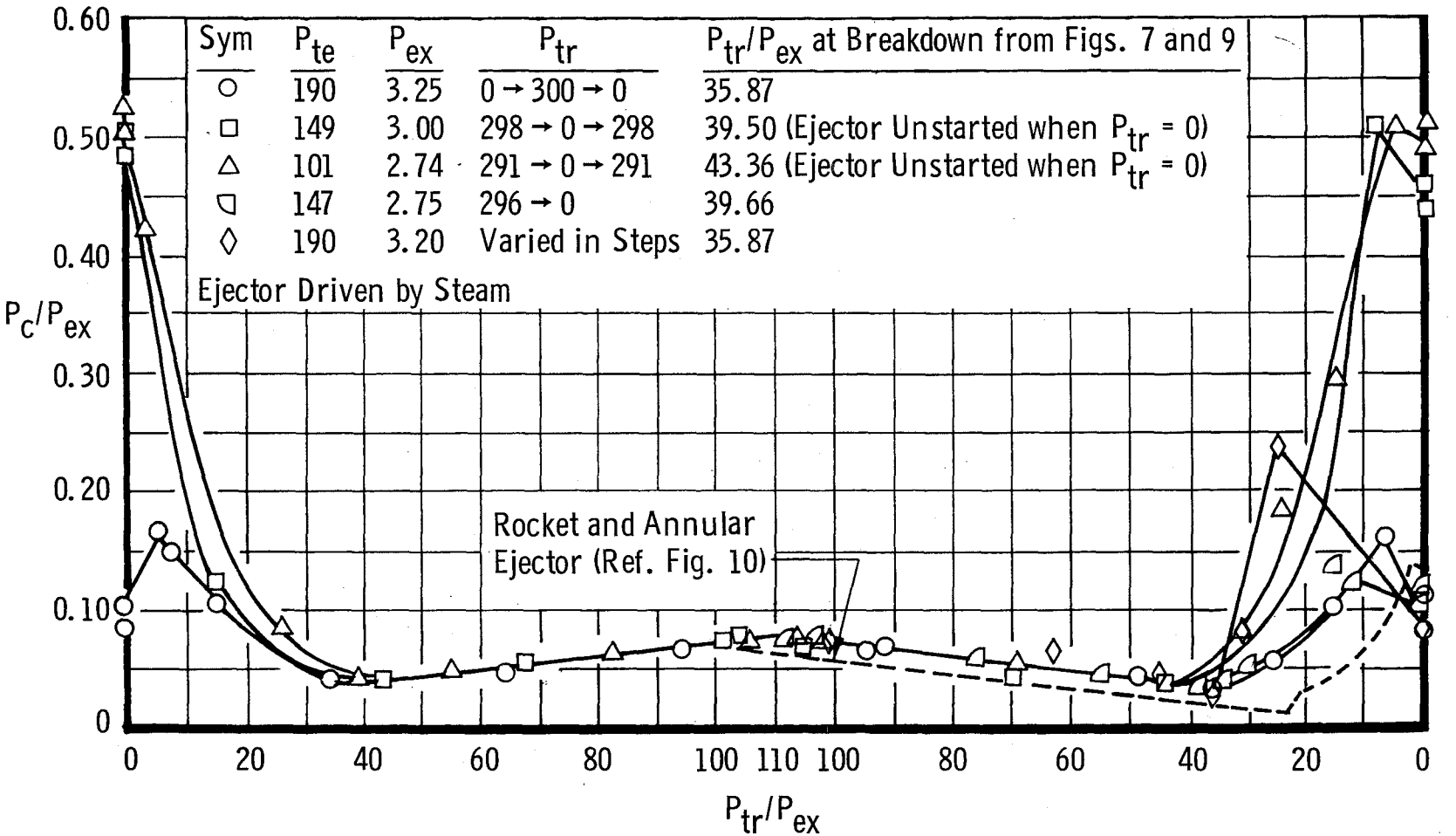

Fig. 14 Air-Driven-Rocket Transient Ignition and Tailoff with Auxiliary Centerbody-Type Ejector